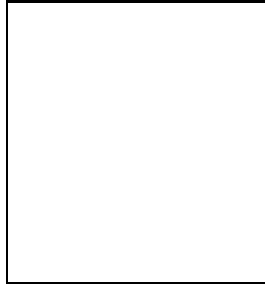


Measurements of Lifetimes, Mixing and CP Violation of B Mesons with the $BABAR$ Detector

G. RAVEN

(for the $BABAR$ collaboration)

*Department of Physics, University of California, San Diego
9500 Gilman Drive, La Jolla, CA 92093*



Using a data sample of 62 million $\Upsilon(4S) \rightarrow B\bar{B}$ decays collected between 1999 and 2001 by the $BABAR$ detector at the PEP-II asymmetric-energy B Factory at SLAC we study events in which one neutral B meson is fully reconstructed in a final state containing a charmonium meson and the flavour of the other neutral B meson is determined from its decay products. The amplitude of the CP -violating asymmetry, which in the Standard Model is proportional to $\sin 2\beta$, is derived from the decay time distributions. We measure $\sin 2\beta = 0.75 \pm 0.09$ (stat) ± 0.04 (syst) and $|\lambda| = 0.92 \pm 0.06$ (stat) ± 0.02 (syst). The latter is consistent with the Standard Model expectation of no direct CP violation. These results are preliminary. In addition, we report on precision measurements of the B lifetimes, and the B^0 - \bar{B}^0 oscillation frequency Δm_d .

1 Introduction

CP violation has been a central concern of particle physics since its discovery in 1964 in the decays of K_L^0 decays¹. An elegant explanation of the CP -violating effects in these decays is provided by the CP -violating phase of the three-generation Cabibbo-Kobayashi-Maskawa (CKM) quark-mixing matrix². However, existing studies of CP violation in neutral kaon decays and the resulting experimental constraints on the parameters of the CKM matrix³ do not provide a stringent test of whether the CKM phase describes CP violation⁴. In the CKM picture, large CP violating asymmetries are expected in the time distributions of B^0 decays to charmonium final states.

In general, CP violating asymmetries are due to the interference between amplitudes with a weak phase difference. For example, a state initially produced as a B^0 (\bar{B}^0) can decay to a CP eigenstate such as $J/\psi K_S^0$ directly or can oscillate into a \bar{B}^0 (B^0) and then decay to $J/\psi K_S^0$. With little theoretical uncertainty in the Standard Model, the phase difference between

these amplitudes is equal to twice the angle $\beta = \arg[-V_{cd}V_{cb}^*/V_{td}V_{tb}^*]$ of the Unitarity Triangle. The CP -violating asymmetry in this mode allows a direct determination of $\sin 2\beta$, and can thus provide a crucial test of the Standard Model.

A $B^0\bar{B}^0$ pair produced in $\Upsilon(4S)$ decays evolves in a coherent P -wave until one of the B mesons decays. If one of the B mesons, referred to as B_{tag} , can be ascertained to decay to a state of known flavour, *i.e.* B^0 or \bar{B}^0 , at a certain time t_{tag} , the other B , referred to as B_{rec} , at *that time* must be of the opposite flavour as a consequence of Bose symmetry. Consequently, the oscillatory probabilities for observing $B^0\bar{B}^0$, B^0B^0 and $\bar{B}^0\bar{B}^0$ pairs produced in $\Upsilon(4S)$ decays are a function of $\Delta t = t_{\text{rec}} - t_{\text{tag}}$, allowing mixing frequency and CP asymmetries to be determined if Δt is known.

At the PEP-II asymmetric e^+e^- collider⁵, resonant production of the $\Upsilon(4S)$ provides a copious source of $B^0\bar{B}^0$ pairs moving along the beam axis (z direction) with an average Lorentz boost of $\langle\beta\gamma\rangle = 0.55$. Therefore, the proper decay-time difference Δt is, to an excellent approximation, proportional to the distance Δz between the two B^0 -decay vertices along the axis of the boost, $\Delta t \approx \Delta z/c\langle\beta\gamma\rangle$. The average separation between the two B decay vertices is $\Delta z \approx \langle\beta\gamma\rangle c\tau_B = 260\ \mu\text{m}$, while the RMS Δz resolution of the detector is about $180\ \mu\text{m}$.

The lifetime, mixing and $\sin 2\beta$ analyses share a common analysis strategy:

- select events where one B , labeled B_{rec} , is fully reconstructed;
- determine the vertex of the other B decay, B_{tag} , in the event by performing a vertex fit to the remaining charged particle trajectories, and compute Δt .

At this point, one can perform an unbinned likelihood fit to the Δt distribution and determine the B lifetime. The mixing and CP asymmetry measurements require one additional step:

- determine the flavour of the B_{tag} decay.

To determine the oscillation frequency Δm_d events are selected where B_{rec} is reconstructed in a neutral decay mode with a known flavour, such as $D^{*+}\pi^-$, and a simultaneous unbinned likelihood fit to the Δt distributions of events where B_{rec} and B_{tag} have opposite flavour (unmixed) and equal flavour (mixed) is performed. To determine CP asymmetries, B_{rec} is a reconstructed CP final state such as $J/\psi K_S^0$, and the Δt distributions of events where B_{tag} is a B^0 and \bar{B}^0 respectively are fitted simultaneously.

In order to establish the experimental technique, we first present precision measurements of the B^0 and B^+ lifetimes, and the $B^0\bar{B}^0$ oscillation frequency Δm_d . These measurements share the same vertexing algorithm and Δt determination as the measurement of the CP asymmetries, and, in case of the mixing measurement, the same flavour tagging algorithm. To eliminate possible experimenter's bias the parameter under study was hidden in all analyses until the event selection and reconstruction, fitting procedure and systematic errors were finalized.

2 The *BABAR* detector and data sets

The data used were recorded with the *BABAR* detector in the period October 1999–December 2001. The total integrated luminosity of the data set is equivalent to $56\ \text{fb}^{-1}$ collected near the $\Upsilon(4S)$ resonance. The corresponding number of produced $B\bar{B}$ pairs is estimated to be about 62 million. The measurement of the charged and neutral B lifetimes is based on the initial 23 million $B\bar{B}$ pairs, whereas the dataset used for the Δm_d measurement includes the first 32 million $B\bar{B}$ pairs. This latter sample was also used for the previously published measurement⁶ of $\sin 2\beta$; in contrast, the preliminary measurement of $\sin 2\beta$ described here utilizes the entire data sample available.

Since the *BABAR* detector is described in detail elsewhere⁷, only a brief description is given here. Surrounding the beam-pipe is a 5-layer silicon vertex tracker (SVT), which provides precise

measurements of the trajectories of charged particles as they leave the e^+e^- interaction point. Outside of the SVT, a 40-layer drift chamber (DCH) allows measurements of track momenta in a 1.5T magnetic field as well as energy-loss measurements, which contribute to charged particle identification. Surrounding the DCH is a detector of internally reflected Cherenkov radiation (DIRC), which provides charged hadron identification. Outside of the DIRC is a CsI(Tl) electromagnetic calorimeter (EMC) that is used to detect photons, provide electron identification and reconstruct neutral hadrons. The EMC is surrounded by a superconducting coil, which creates the magnetic field for momentum measurements. Outside of the coil, the flux return is instrumented with resistive plate chambers interspersed with iron (IFR) for the identification of muons and long-lived neutral hadrons. We use the GEANT4 package⁸ to simulate interactions of particles traversing the *BABAR* detector.

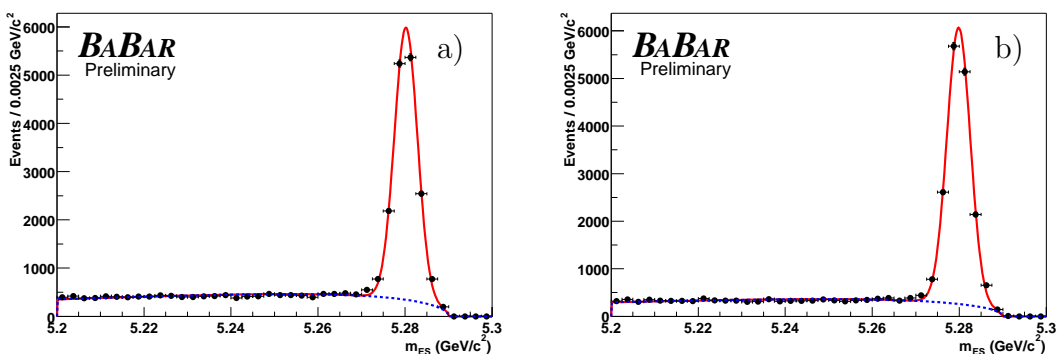
3 Measurement of B Lifetimes and Δm_d

3.1 Exclusive B reconstruction

The so-called B_{flav} sample used for lifetime and mixing analyses consists of events where B_{rec} is reconstructed in the modes $B^0 \rightarrow D^{(*)-}\pi^+$, $D^{(*)-}\rho^+$, $D^{(*)-}a_1^+$, $J/\psi K^{*0}$ and $B^+ \rightarrow \bar{D}^{(*)0}\pi^+$, $J/\psi K^+$, $\psi(2S)K^+$. Charged and neutral \bar{D}^* candidates are formed by combining a \bar{D}^0 with a π^- or π^0 . \bar{D}^0 candidates are reconstructed in the decay channels $K^+\pi^-$, $K^+\pi^-\pi^0$, $K^+\pi^+\pi^-\pi^-$ and $K_S^0\pi^+\pi^-$ and D^- candidates in the decay channels $K^+\pi^-\pi^-$ and $K_S^0\pi^-$. We reconstruct J/ψ and $\psi(2S)$ in the decays to e^+e^- and $\mu^+\mu^-$ and the $\psi(2S)$ decay to $J/\psi \pi^+ \pi^-$.

Continuum $e^+e^- \rightarrow q\bar{q}$ background is suppressed by requirements on the normalized second Fox-Wolfram moment⁹ for the event and on the angle between the thrust axes of B_{rec} and of the other B in the event. B_{rec} candidates are identified by the difference ΔE between the reconstructed B energy and $\sqrt{s}/2$ in the $\Upsilon(4S)$ frame, and the beam-energy substituted mass m_{ES} calculated from $\sqrt{s}/2$ and the reconstructed B momentum. We require $m_{\text{ES}} > 5.2 \text{ GeV}/c^2$ and $|\Delta E| < 3\sigma_{\Delta E}$. The distributions of m_{ES} for selected B_{flav} candidates is shown in Fig. 1.

Figure 1: Beam energy substituted mass distribution for selected B^0 (a) and B^+ (b) candidates. In 56 fb^{-1} , we reconstruct 15K B^0 and 13K B^+ flavour tagged signal events. Average signal purities for $m_{\text{ES}} > 5.27 \text{ GeV}/c^2$, are 85 % and 89 %, respectively.



3.2 Δt determination

The decay time difference, Δt , between the two B decays is determined from the measured separation, $\Delta z = z_{\text{rec}} - z_{\text{tag}}$, along the z axis between the reconstructed B_{rec} (z_{rec}) and flavour-tagging decay B_{tag} vertex (z_{tag}). This measured Δz is converted into Δt with the known $\Upsilon(4S)$ boost, including a correction on an event-by-event basis for the direction of the B mesons

with respect to the z direction in the $\Upsilon(4S)$ frame. The Δt resolution is limited by the z resolution of the tagging vertex. The B_{tag} decay vertex reconstruction starts from all tracks in the event except those incorporated in B_{rec} . An additional constraint is provided by the calculated B_{tag} production point and three-momentum, determined from the three-momentum of the fully reconstructed B_{rec} candidate, its decay vertex, and the average position of the interaction point (with a vertical size of $10\ \mu\text{m}$) and the $\Upsilon(4S)$ average boost. The derived B_{tag} trajectory is fit to a common vertex with the remaining tracks in the event. Reconstructed K_S^0 or Λ candidates are used as input to the fit in place of their daughters in order to reduce bias due to long-lived particles. Tracks with a large contribution to the χ^2 are iteratively removed from the fit until all remaining tracks have a reasonable fit probability or all tracks are removed. For 99.5% of the reconstructed events the r.m.s Δz resolution is $180\ \mu\text{m}$.

Two different parameterizations are used to model the decay-time difference resolution. In the measurements of Δm_d and $\sin 2\beta$, the time resolution function is approximated by a sum of three Gaussian distributions (core, tail, and outlier) with different means and widths,

$$\mathcal{R}(\delta_t, \sigma_{\Delta t}; \hat{a} = \{f_k, S_k, b_k, \sigma_3\}) = \sum_{k=1}^2 \frac{f_k}{S_k \sigma_{\Delta t} \sqrt{2\pi}} \exp\left(-\frac{(\delta_t - b_k \sigma_{\Delta t})^2}{2(S_k \sigma_{\Delta t})^2}\right) + \frac{f_3}{\sigma_3 \sqrt{2\pi}} \exp\left(-\frac{\delta_t^2}{2\sigma_3^2}\right), \quad (1)$$

where $\delta_t = \Delta t - \Delta t_{\text{true}}$. For the core and tail Gaussians, the widths $\sigma_k = S_k \times \sigma_{\Delta t}$ are the event-by-event measurement errors scaled by a common factor S_k . The scale factor of the tail Gaussian is fixed to the Monte Carlo value since it is strongly correlated with the other resolution function parameters. The third Gaussian, with a fixed width of $\sigma_3 = 8\ \text{ps}$, accounts for outlier events with incorrectly reconstructed vertices (less than 1% of events). The offsets b_i are modeled to be proportional to $\sigma_{\Delta t}$, which is correlated with the weight that the remaining daughters of charm particles have in the tag vertex reconstruction. The tail and outlier fractions and the scale factors are assumed to be the same for all decay modes, since the precision of the B_{tag} vertex measurement is the limiting factor for the Δt resolution. This assumption is confirmed by Monte Carlo studies.

The three Gaussian resolution function is less suited for the measurements of B lifetimes due to the large correlation between the resolution function parameters and the lifetimes, which leads to increased statistical errors. Studies with Monte Carlo simulations and data show that the sum of a zero-mean Gaussian distribution and its convolution with a one-sided exponential provides a good trade-off between statistical and systematic uncertainties in the lifetime measurement:

$$\mathcal{R}(\delta_t, \sigma_{\Delta t} | \hat{a} = \{f_1, s, \kappa\}) = f_1 \frac{1}{\sqrt{2\pi} s \sigma_{\Delta t}} \exp\left(-\frac{\delta_t^2}{2s^2 \sigma_{\Delta t}^2}\right) + \int_{-\infty}^0 \frac{1 - f_1}{\kappa \sigma_{\Delta t}} \exp\left(\frac{\delta'_t}{\kappa \sigma_{\Delta t}}\right) \frac{1}{\sqrt{2\pi} s \sigma_{\Delta t}} \exp\left(-\frac{(\delta_t - \delta'_t)^2}{2s^2 \sigma_{\Delta t}^2}\right) d(\delta'_t). \quad (2)$$

The parameters \hat{a} are the fraction f in the core Gaussian component, a scale factor s for the per-event errors $\sigma_{\Delta t}$, and the factor κ in the effective time constant $\kappa \sigma_{\Delta t}$ of the exponential which accounts for charm decays. Δt outlier events are modeled the same way as in the three Gaussian resolution function. The resolution functions differ only slightly between B^0 and B^+ mesons due to different mixtures of D^- and \bar{D}^0 mesons in the B_{tag} decays and we use a single set of resolution function parameters for both B^0 and B^+ in the lifetime fits.

3.3 Lifetime results

We extract the B^+ and B^0 lifetimes from an unbinned maximum likelihood fit to the Δt distributions of the selected B candidates. The probability for an event to be signal is estimated from

m_{ES} fits (Fig. 1) and the m_{ES} value of the B_{rec} candidate. In the likelihood, the probability density for the signal events is given by

$$\mathcal{G}(\Delta t, \sigma_{\Delta t} | \tau, \hat{a}) = \int_{-\infty}^{+\infty} e^{-|\Delta t|/\tau} / (2\tau) \mathcal{R}(\Delta t - \Delta t', \sigma_{\Delta t} | \hat{a}) d(\Delta t'), \quad (3)$$

and the background Δt distribution for each B species is empirically modeled by the sum of a prompt component and a lifetime component convolved with the same resolution function, but with a separate set of parameters. The likelihood fit involves 17 free parameters in addition to the B^0 and the B^+ lifetimes: 12 to describe the background Δt distributions and 5 for the signal resolution function. The charged B lifetime τ_{B^+} is replaced with $\tau_{B^+} = r \cdot \tau_{B^0}$ to estimate the statistical error on the ratio $r = \tau_{B^+} / \tau_{B^0}$.

We determine the B^0 and B^+ meson lifetimes and their ratio to be:

$$\begin{aligned} \tau_{B^0} &= 1.546 \pm 0.032 \text{ (stat)} \pm 0.022 \text{ (syst)} \text{ ps,} \\ \tau_{B^+} &= 1.673 \pm 0.032 \text{ (stat)} \pm 0.023 \text{ (syst)} \text{ ps, and} \\ \tau_{B^+} / \tau_{B^0} &= 1.082 \pm 0.026 \text{ (stat)} \pm 0.012 \text{ (syst).} \end{aligned}$$

These are the most precise published measurements to date¹⁰ and are consistent with the world averages¹¹. The resolution function parameters are consistent with those found in a Monte Carlo simulation that includes detector alignment effects. With the current data sample these measurements are still statistically limited. The dominant systematic errors arise from uncertainties in the description of the combinatorial background and of events with large Δt values, the use of a common time resolution function for B^0 and B^+ and from limited Monte Carlo statistics.

3.4 Flavour tagging

After the daughter tracks of the B_{rec} are removed from the event, the remaining tracks are analyzed to determine the flavour of the B_{tag} , and this ensemble is assigned a tag flavour, either B^0 or \bar{B}^0 . For this purpose, flavour tagging information carried by primary leptons from semileptonic B decays, charged kaons, soft pions from D^* decays, and more generally by high momentum charged particles is used to uniquely assign an event to a tagging category.

Events are assigned a **Lepton** tag if they contain an identified lepton with a center-of-mass momentum greater than 1.0 or 1.1 GeV/ c for electrons and muons, respectively. The momentum requirement selects mostly primary leptons by suppressing opposite-sign leptons from semileptonic charm decays. If the sum of charges of all identified kaons is non-zero, the event is assigned a **Kaon** tag. The final two tags involve a multi-variable analysis based on a neural network, which is trained to identify primary leptons, kaons, and soft pions, and the momentum and charge of the track with the maximum center-of-mass momentum. Depending on the output of the neural net, events are assigned either an NT1 (more certain) tag, an NT2 (less certain) tag, or are considered not tagged (about 30% of events) and excluded from the analysis. The tagging power of the NT1 and NT2 tags comes primarily from slow pions, from kinematically recovering non-identified primary electrons and muons, and from kaons that do not pass the selection criteria for the **Kaon** category.

Tagging assignments are made mutually exclusive by the hierarchical use of the tags. Events with a **Lepton** tag and no conflicting **Kaon** tag are assigned to the **Lepton** category. If no **Lepton** tag exists, but the event has a **Kaon** tag, it is assigned to the **Kaon** category. Otherwise the event is assigned to one of the two neural network categories.

The effective tagging efficiency $Q_i = \varepsilon_i(1 - 2w_i)^2$, where ε_i is the fraction of events assigned to category i and w_i the probability of obtaining a wrong tag, is used as the basis for optimization of category selection criteria. The statistical errors on Δm_d and $\sin 2\beta$ are proportional to $1/\sqrt{Q}$, where $Q = \sum Q_i$. The contributions of the various tagging categories to Q is shown in Table 1.

Table 1: Tagging efficiency ε , average mistag fractions w , mistag differences $\Delta w = w(B^0) - w(\bar{B}^0)$, and the derived Q (defined in the text) obtained from the likelihood fit to the B_{flav} and B_{CP} samples.

Category	ε (%)	w (%)	Δw (%)	Q (%)
Lepton	11.1 ± 0.2	8.6 ± 0.9	0.6 ± 1.5	7.6 ± 0.4
Kaon	34.7 ± 0.4	18.1 ± 0.7	-0.9 ± 1.1	14.1 ± 0.6
NT1	7.7 ± 0.2	22.0 ± 1.5	1.4 ± 2.3	2.4 ± 0.3
NT2	14.0 ± 0.3	37.3 ± 1.3	-4.7 ± 1.9	0.9 ± 0.2
All	67.5 ± 0.5			25.1 ± 0.8

3.5 Mixing result

The value of Δm_d is extracted from the tagged flavour-eigenstate B^0 sample with a simultaneous unbinned likelihood fit to the Δt distributions of both unmixed and mixed events. The PDFs for the unmixed (+) and mixed (−) signal events for the i^{th} tagging category are given by

$$\mathcal{H}_{\pm}(\Delta t, \sigma_{\Delta t} | \Delta m_d, w_i, \hat{a}_i) = \frac{e^{-|\Delta t|/\tau}}{4\tau} [1 \pm (1 - 2w_i) \cos \Delta m_d \Delta t] \otimes \mathcal{R}(\delta_t, \sigma_{\Delta t} | \hat{a}_i). \quad (4)$$

Some resolution function parameters are allowed to differ for each tagging category to account for shifts due to inclusion of charm decay products in the tag vertex. The PDFs are extended to include background terms, different for each tagging category. The probability that a B^0 candidate is a signal event is determined from a fit to the observed m_{ES} distribution for its tagging category. The Δt distributions of the combinatorial background are described with a zero lifetime component and a non-oscillatory component with non-zero lifetime. Separate resolution function parameters are used for signal and background to minimize correlations.

The Δt distributions of the signal ($m_{\text{ES}} > 5.27 \text{ GeV}/c^2$) overlaid with the projections of the likelihood fit, are shown in Fig. 2. In addition, the mixing asymmetry,

$$\mathcal{A}_{\text{mix}}(\Delta t) = \frac{N_{\text{unmixed}}(\Delta t) - N_{\text{mixed}}(\Delta t)}{N_{\text{unmixed}}(\Delta t) + N_{\text{mixed}}(\Delta t)}. \quad (5)$$

is plotted. If flavour tagging and Δt determination were perfect, the asymmetry as a function of Δt would be a cosine with unit amplitude.

The probability to obtain a likelihood smaller than that observed is 44%, evaluated with a parameterized Monte Carlo technique. The value of Δm_d obtained is

$$\Delta m_d = 0.516 \pm 0.016(\text{stat}) \pm 0.010(\text{syst}) \text{ ps}^{-1}. \quad (6)$$

Since the parameters of the Δt resolution and the mistag rates w are free parameters in the fit, their contribution to the uncertainty on Δm_d is included as part of the statistical error. The main contributions to the systematic errors are the choice of the signal Δt resolution description, its capability to handle outliers and various worst-case SVT misalignment scenarios ($\pm 0.005 \text{ ps}^{-1}$), and by correlations between mistag rates and Δt resolution which are not explicitly modeled by the likelihood fit ($\pm 0.005 \text{ ps}^{-1}$). Finally, the variation of the fixed B^0 lifetime within known errors¹¹ leads to a systematic uncertainty of $\pm 0.006 \text{ ps}^{-1}$.

This is one of the single most precise mixing measurements available¹², and is consistent with the current world average¹¹.

4 Determination of $\sin 2\beta$

For the measurement of $\sin 2\beta$, B_{rec} is fully reconstructed in a CP eigenstate with eigenvalue $\eta_{CP} = -1$ ($J/\psi K_S^0$, $\psi(2S)K_S^0$, or $\chi_{c1}K_S^0$) or $+1$ ($J/\psi K_L^0$), while B_{tag} is tagged just as for the

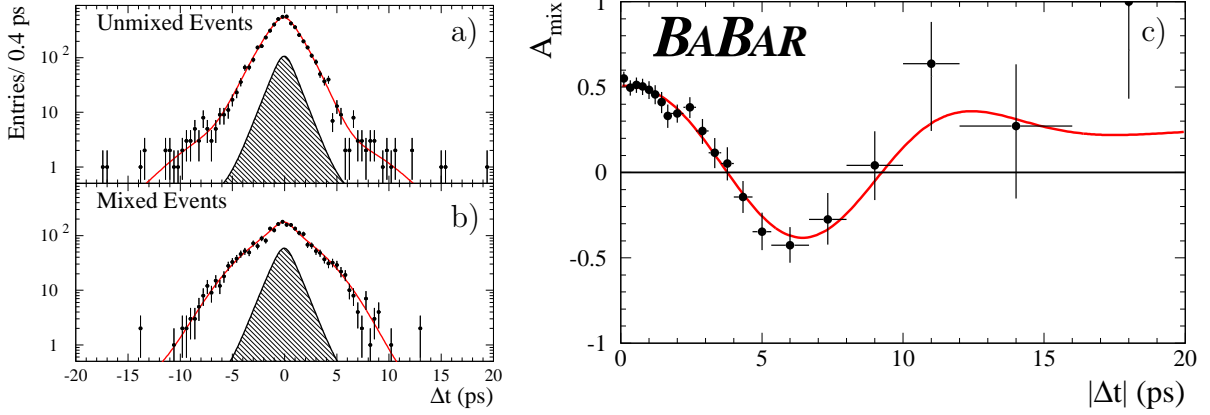


Figure 2: Distributions of Δt for (a) unmixed and (b) mixed events in the signal region $m_{ES} > 5.27 \text{ GeV}/c^2$. The data points are overlaid with the result from the fit, projected using the individual signal probabilities and event-by-event Δt resolutions, along with the simultaneously determined background distribution. Also shown (c) is the time-dependent mixing asymmetry $\mathcal{A}_{mix}(|\Delta t|)$ defined in the text.

mixing measurement. The sample is further enlarged by including the mode $J/\psi K^{*0}$ ($K^{*0} \rightarrow K_S^0 \pi^0$). However, due to the presence of even ($L = 0, 2$) and odd ($L = 1$) orbital angular momenta in the $J/\psi K^{*0}$ system, there are $\eta_{CP} = -1$ and $+1$ contributions to its decay rate. These contributions are disentangled by incorporating their dependence on the transversity angles in each event into the likelihood fit¹³. The m_{ES} distributions (ΔE for $J/\psi K_L^0$) of the selected sample are shown in Fig. 3, and the detailed breakdown in Table 2.

Table 2: Number of tagged events, signal purity, and result of fitting for CP asymmetries in the full CP sample and in various subsamples, as well as in the B_{flav} and charged B control samples. Purity is the fitted number of signal events divided by the total number of events in the ΔE and m_{ES} signal region defined in the text.

Sample	N_{tag}	Purity (%)	$\sin 2\beta$
Full CP sample	1850	79	0.75 ± 0.09
$J/\psi K_S^0$ ($K_S^0 \rightarrow \pi^+ \pi^-$)	693	96	0.79 ± 0.11
$J/\psi K_S^0$ ($K_S^0 \rightarrow \pi^0 \pi^0$)	123	89	0.42 ± 0.33
$\psi(2S)K_S^0$	119	89	0.84 ± 0.32
$\chi_{c1}K_S^0$	60	94	0.84 ± 0.49
$J/\psi K_L^0$	742	57	0.73 ± 0.19
$J/\psi K^{*0}$ ($K^{*0} \rightarrow K_S^0 \pi^0$)	113	83	0.62 ± 0.56
$J/\psi K_S^0, \psi(2S)K_S^0, \chi_{c1}K_S^0$ only ($\eta_f = -1$)	995	94	0.76 ± 0.10
Lepton tags	176	97	0.73 ± 0.16
Kaon tags	504	95	0.75 ± 0.14
NT1 tags	117	95	0.86 ± 0.33
NT2 tags	198	94	0.84 ± 0.61
B^0 tags	471	94	0.79 ± 0.14
\bar{B}^0 tags	524	95	0.73 ± 0.14
B_{flav} sample	17546	85	0.00 ± 0.03
Charged B sample	14768	89	-0.02 ± 0.03

The decay-time distribution of B decays to a CP eigenstate with a B^0 or \bar{B}^0 tag can be expressed in terms of a complex parameter λ that depends on both the B^0 - \bar{B}^0 oscillation amplitude and the amplitudes describing \bar{B}^0 and B^0 decays to this final state¹⁴. The decay rate

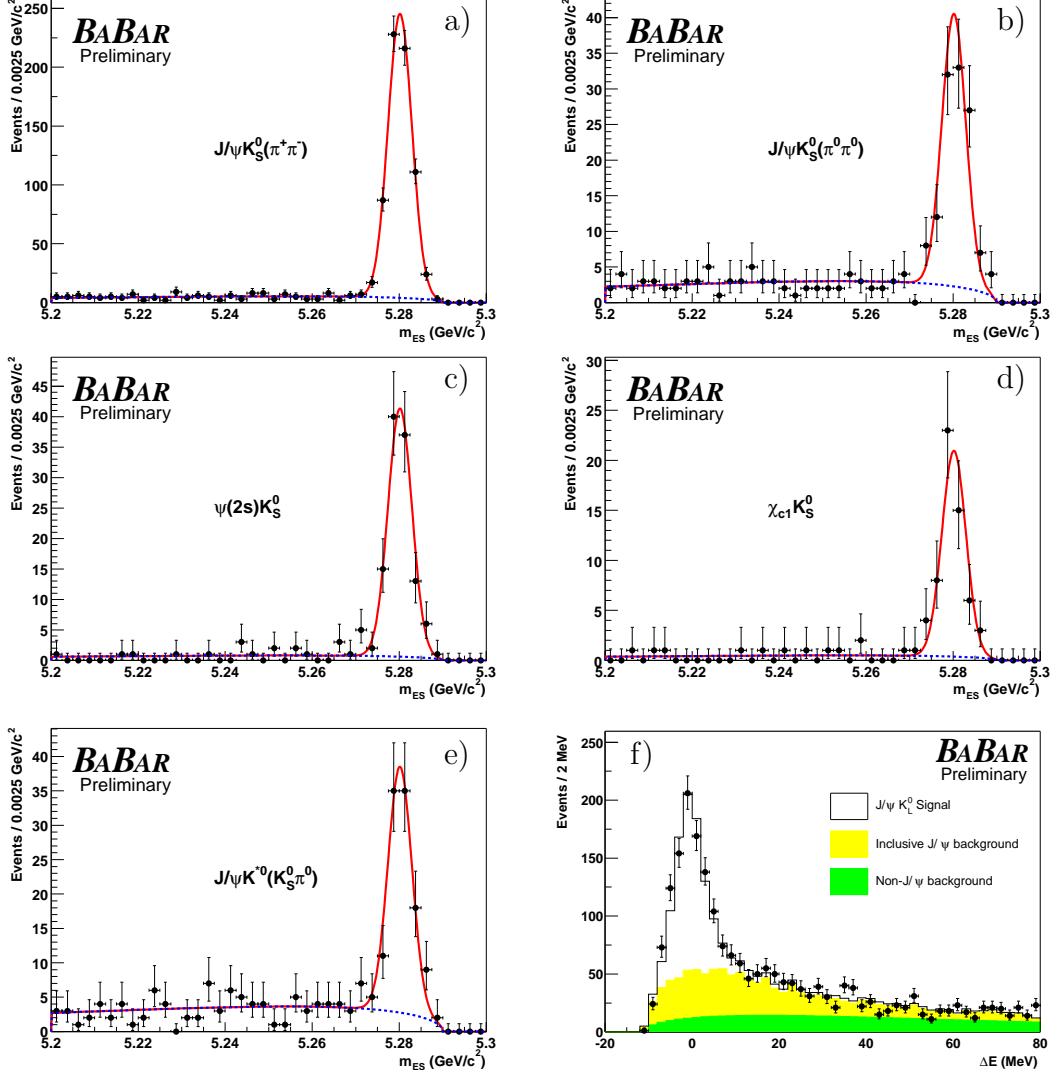


Figure 3: Distribution of m_{ES} for flavour tagged B_{CP} candidates selected in the final states a) $J/\psi K_S^0$ ($K_S^0 \rightarrow \pi^+ \pi^-$), b) $J/\psi K_S^0$ ($K_S^0 \rightarrow \pi^0 \pi^0$), c) $\psi(2S)K_S^0$, d) $\chi_{c1}K_S^0$, e) $J/\psi K^{*0}$ ($K^{*0} \rightarrow K_S^0 \pi^0$), and f) distribution of ΔE for flavour tagged $J/\psi K_L^0$ candidates.

$\mathcal{F}_+(\mathcal{F}_-)$ when the tagging meson is a $B^0(\bar{B}^0)$ is given by

$$\begin{aligned}
& \mathcal{F}_\pm(\Delta t, \sigma_{\Delta t} | \sin 2\beta, w_i, \hat{a}_i) \\
&= \frac{e^{-|\Delta t|/\tau_{B^0}}}{4\tau_{B^0}} \left[1 \pm (1 - 2w_i) \left(\frac{2\text{Im}\lambda}{1 + |\lambda|^2} \sin(\Delta m_d \Delta t) - \frac{1 - |\lambda|^2}{1 + |\lambda|^2} \cos(\Delta m_d \Delta t) \right) \right] \\
&\otimes \mathcal{R}(\delta_t, \sigma_{\Delta t} | \hat{a}_i),
\end{aligned} \tag{7}$$

where the + or - sign indicates whether the B_{tag} is tagged as a B^0 or a \bar{B}^0 , respectively.

The distributions are much simpler when $|\lambda| = 1$, which is the expectation of the Standard Model for decays like $B^0 \rightarrow J/\psi K_S^0$ where all amplitudes which contribute to the decay have the same weak phase. In this particular case one is left with the phase difference introduced by B^0 - \bar{B}^0 mixing, i.e. $\lambda = \eta_{CP} e^{2i\beta}$, where η_{CP} is the CP eigenvalue of the final state.

It is possible to construct a CP -violating observable which, neglecting resolution effects, is proportional to $\sin 2\beta$:

$$\mathcal{A}_{CP}(\Delta t) = \frac{\mathcal{F}_+(\Delta t) - \mathcal{F}_-(\Delta t)}{\mathcal{F}_+(\Delta t) + \mathcal{F}_-(\Delta t)} \propto -\eta_{CP}(1 - 2w) \sin 2\beta \sin \Delta m_d \Delta t. \tag{8}$$

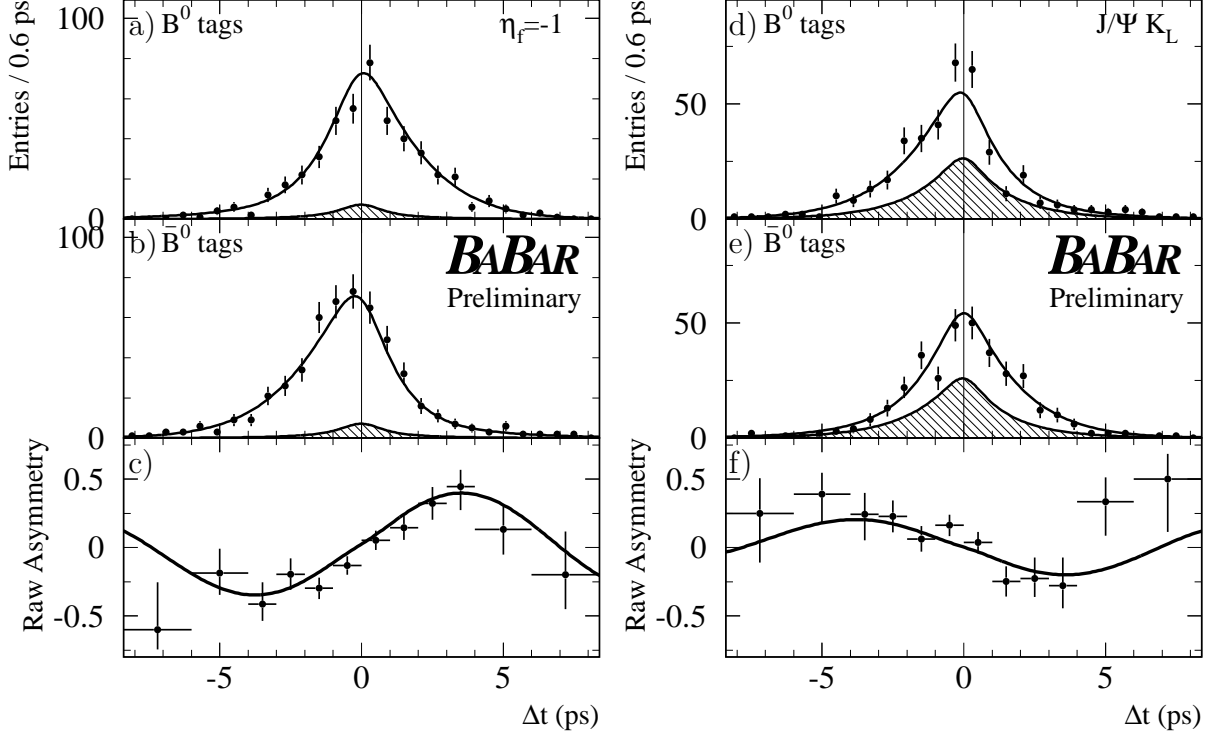


Figure 4: Number of $\eta_f = -1$ candidates ($J/\psi K_S^0$, $\psi(2S)K_S^0$, $\chi_{c1}K_S^0$) in the signal region a) with a B^0 tag N_{B^0} and b) with a \bar{B}^0 tag $N_{\bar{B}^0}$, and c) the raw asymmetry $(N_{B^0} - N_{\bar{B}^0})/(N_{B^0} + N_{\bar{B}^0})$, as functions of Δt . The solid curves represent the result of the combined fit to the full B_{CP} sample. The shaded regions represent the background contributions. Figures d) – f) contain the corresponding information for the $\eta_f = +1$ mode $J/\psi K_L^0$. The likelihood is normalized to the total number of B^0 and \bar{B}^0 tags. The value of $\sin 2\beta$ is independent of the individual normalizations and therefore of the difference between the number of B^0 and \bar{B}^0 tags. This difference is responsible for the small vertical shift between the data points and the solid curves.

Since no time-integrated CP asymmetry effect is expected, an analysis of the time-dependent asymmetry is necessary. The interference between the two amplitudes, and hence the CP asymmetry, is maximal after approximately 2.1 B^0 proper lifetimes, when the mixing asymmetry goes through zero. However, the maximum sensitivity to $\sin 2\beta$, which is proportional to $e^{-\Gamma\Delta t} \sin^2 \Delta m_d \Delta t$, occurs in the region of 1.4 lifetimes.

The value of $\sin 2\beta$ can be extracted by maximizing the likelihood function

$$\ln \mathcal{L}_{CP} = \sum_i^{\text{tagging}} \left[\sum_{B^0 \text{ tag}} \ln \mathcal{F}_+(\Delta t, \sigma_{\Delta t}; \sin 2\beta, w_i, \hat{a}_i,) + \sum_{\bar{B}^0 \text{ tag}} \ln \mathcal{F}_-(\Delta t, \sigma_{\Delta t}; \sin 2\beta, w_i, \hat{a}_i,) \right], \quad (9)$$

where the outer summation is over tagging categories i and the inner summations are over the B^0 and \bar{B}^0 tags within a given tagging category. In practice, the fit for $\sin 2\beta$ is performed on the combined B_{flav} and B_{CP} samples with a likelihood constructed from the sum of Eq. 4 and 9, in order to determine $\sin 2\beta$, the mistag fraction w_i for each tagging category, and the resolution parameters \hat{a}_i simultaneously. Additional terms are included in the likelihood to account for backgrounds and their time dependence. The determination of the mistag fractions and Δt resolution function for the signal is dominated by the high-statistics B_{flav} sample. We fix $\tau_{B^0} = 1.548 \text{ ps}$ and $\Delta m_d = 0.472 \text{ ps}^{-1}$ ¹¹. The largest correlation between $\sin 2\beta$ and any linear combination of other free parameters is only 0.14.

The simultaneous fit to all CP decay modes and the flavour decay modes yields:

$$\sin 2\beta = 0.75 \pm 0.09(\text{stat}) \pm 0.04(\text{syst}). \quad (10)$$

The dominant sources of systematic uncertainties are the choice of parameterization of the Δt resolution function, possible differences in the mistag fractions between the CP sample and the flavour sample, and uncertainties in the level, composition and CP asymmetry of the background in the selected events. The large sample of fully reconstructed events allows a number of consistency checks, including separation of the data by decay mode, tagging category and B_{tag} flavour.

This analysis¹³ improves upon and supercedes the previously published result⁶. It provides the single most precise measurement of $\sin 2\beta$ currently available and is consistent with the range implied by indirect measurements and theoretical estimates of the magnitudes of CKM matrix elements in the context of the Standard Model¹⁵.

References

1. J.H. Christenson *et al.*, Phys. Rev. Lett. **13**, 138 (1964); NA31 Collaboration, G.D. Barr *et al.*, Phys. Lett. **317**, 233 (1993); E731 Collaboration, L.K. Gibbons *et al.*, Phys. Rev. Lett. **70**, 1203 (1993).
2. N. Cabibbo, Phys. Rev. Lett. **10**, 531 (1963); M. Kobayashi and T. Maskawa, Prog. Th. Phys. **49**, 652 (1973).
3. See, for instance, “Overall determinations of the CKM matrix”, Section 14 in “The *BABAR* physics book”, P. H. Harrison and H. R. Quinn, eds., SLAC-R-504 (1998), and references therein.
4. For an introduction to CP violation, see, for instance, “A CP violation primer”, Section 1 in “The *BABAR* physics book”, *op. cit.*³, and references therein.
5. “PEP-II: An Asymmetric B Factory”, Conceptual Design Report, SLAC-418, LBL-5379 (1993).
6. *BABAR* Collaboration, B. Aubert *et al.*, Phys. Rev. Lett. **87**, 091801; *BABAR* Collaboration, B. Aubert *et al.*, *BABAR*-PUB-01/03, SLAC-PUB-9060, hep-ex/0201020, to appear in Phys. Rev. D.
7. *BABAR* Collaboration, B. Aubert *et al.*, Nucl. Instr. and Methods **A479**, 117 (2002).
8. <http://wwwinfo.cern.ch/asd/geant4/geant4.html>
9. G.C. Fox and S. Wolfram, Phys. Rev. Lett. **41**, 1581 (1978).
10. *BABAR* Collaboration, B. Aubert *et al.*, Phys. Rev. Lett. **87**, 201803
11. Particle Data Group, D.E. Groom *et al.*, Eur. Phys. Jour. C **15**, 1 (2000).
12. *BABAR* Collaboration, B. Aubert *et al.*, *BABAR*-PUB-01/02, SLAC-PUB-9061, hep-ex/0112044, to appear in Phys. Rev. Lett..
13. *BABAR* Collaboration, B. Aubert *et al.*, *BABAR*-CONF-02/01, SLAC-PUB-9153, hep-ex/0203007.
14. See, for example, L. Wolfenstein, Eur. Phys. Jour. C **15**, 115 (2000).
15. See, for example, F.J. Gilman, K. Kleinknecht and B. Renk, Eur. Phys. Jour. C **15**, 110 (2000).

This figure "picture.jpg" is available in "jpg" format from:

<http://arxiv.org/ps/hep-ex/0205045v1>